

Pulsed electrodeposition of metals into porous anodic alumina

A.N. Belov · S.A. Gavrilov · V.I. Shevyakov ·
E.N. Redichev

Received: 29 March 2010 / Accepted: 22 June 2010 / Published online: 30 July 2010
© Springer-Verlag 2010

Abstract A detailed analysis of the optimum regimes of pulsed current metal electrodeposition into pores of porous anodic alumina PAA is presented. A simple model based on cathodic and anodic current transients is developed. The model is based on a simplified equivalent circuit consisting of two capacities related to the barrier and porous parts of porous anodic alumina. Nanowires of Cd, Zn, In, Ni, Co, Ag, and Cu were embedded into PAA by pulsed electrodeposition using an asymmetric rectangular ac signal. Deposited metal nanowires were characterized by scanning electron microscopy (SEM), atomic force microscopy (AFM), optical spectroscopy, Auger electron spectroscopy (AES), and X-ray diffractometry (XRD).

1 Introduction

Recently the interest in the fabrication of one-dimensional nanostructures has been increasing because of their potential use in high-density magnetic memories [1, 2], single-electron devices [3], nanoelectrodes for the direct gas phase deposition of nanoparticles [4], and optical media fabrication [5]. These structures may be prepared by vapor–solid growth, carbothermal reactions, etc. [6]. Electrochemical

deposition of nanowires in porous templates of porous silicon and track-etched polycarbonate is used by many researchers for fabricating a wide variety of nanowire arrays. From this point of view porous anodic alumina (PAA) is the most promising template. A periodic pore arrangement in porous anodic alumina was reported by many authors [7–9]. Various metals [10], metal oxides [11], and metal chalcogenides [12] were successfully electrodeposited into nanopores of PAA. However, device structures based on nanowires deposited into PAA are not made yet, probably due to problems of making high-quality nanowire formation a common technological process. The electrochemical deposition of nanowires into PAA is usually performed under direct current (dc) regime. Therefore, the PAA needs to be detached from the aluminum substrate. Subsequently, the barrier layer is removed from the matrix structure with a chemical etching process. As a final pretreatment step for the filling process, a metallic contact evaporates on one side of a free-standing alumina membrane [13]. However, these PAA membranes are very brittle and unsuitable for further thermal processing and mechanical operations.

One can overcome the problem of low mechanical stability of PAA membranes by leaving them on the Al-substrate, for example, by using Al films sputtered on conducting indium-tin oxides (ITO) [14]. However, adhesion between PAA and ITO substrate may be a serious problem for further processing. In this work, ac electrochemical deposition has been applied to nanowire formation in PAA. The advantage of ac electrochemical deposition is that the membrane remains on the Al substrate and that the barrier layer does not avoid the deposition. In this case, the production of ordered and metal-filled PAA structures is not limited by the thickness and size of the PAA layer. These structures may be used in high-temperature technological operations. First ac electrodeposition of Cu, Ni, Co, and Sn was reported in [10].

A.N. Belov (✉) · S.A. Gavrilov · V.I. Shevyakov
Moscow Institute of Electronic Technology, Technical University,
4806-th street 5, Zelenograd, Moscow, Russia
e-mail: belov@dtd.miee.ru
Fax: +7-495-5329932

E.N. Redichev
Research-and-manufacturing firm “NanoInTech”, Sosnovaya
alley 6, Zelenograd, Moscow, Russia
e-mail: info@nanointech.ru

Metal array deposition into the PAA templates was carried out by sine-wave ac of 50 Hz. More homogeneous filling of pores by metal was made in [15] in nonsymmetric pulsed regime. However, there was no detail analysis of the regimes used for deposition.

We had offered short results of investigation pulsed electrodeposition method of metals in [16]. In this work we presented more comprehensive data about this investigation.

2 Experiments

PAA films were formed by two-stage anodization of aluminium foil 99% purity (thickness 100 μm). First one-hour stage was performed in 1 M aqueous solution of $(\text{COOH})_2$ under 10 mA/cm^2 current density. During the process, the voltage measured between a pattern and stainless steel electrode was 50 V. The layer of anodic oxide was removed by etching in water solution of 0.35 M H_3PO_4 and 0.2 M CrO_3 at 90°C before second anodization that was performed with the same conditions. After one-hour anodization, every 5 minutes, current density was reduced down to 5, 2.5, 1.2, 0.6 mA/cm^2 followed by anodizing voltage decreased from 50 to 8 V that may be interpreted as thinning of barrier layer from 55 to 8 nm [17].

Various metals were electrochemically deposited into pores by supplying nonsymmetrical rectangular voltage pulses. Russian G5-79 generator is used as power supply with maximum supplied voltage of 10 V. Deposition was performed until metal film appeared on the oxide surface. Then the metal film was removed with polishing material. After that, the film was washed properly by deionized water and then dried in nitrogen flow.

The deposited structures were examined by AFM, SEM, optical spectroscopy AES, and XRD.

3 Results and discussion

A model based on regular oxide structure was developed for optimizing electrochemical metal deposition into pores of PAA. Schematically PAA can be presented as an array of regular pores in anodic alumina that was separated from aluminium substrate by barrier oxide layer (Fig. 1).

From physical point of view, PAA may be considered to be a system consisting of conductive electrolyte, aluminum wafer, and insulating aluminum oxide.

The ac equivalent electrical circuit of the system consists of parallelly connected capacitors C_p and C_b that present capacities of porous and barrier layers (Fig. 2). The capacities may be estimated by the following equations:

$$C_p = \frac{\varepsilon\varepsilon_0 S_{ox}}{d_p}, \quad C_b = \frac{\varepsilon\varepsilon_0 S_b}{d_b}, \quad (1)$$

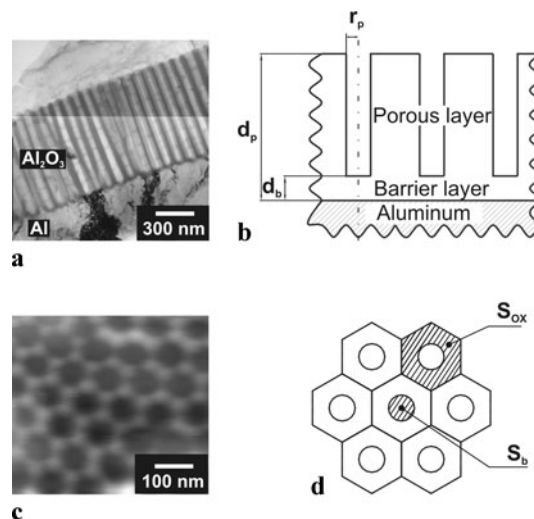
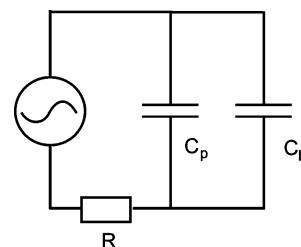


Fig. 1 SEM image of cross-section (a), AFM image of surface (c), and schemes of PAA (b, d)

Fig. 2 Ac equivalent electrical circuit of the PAA



where S_{ox} is the surface area of porous part of the oxide, S_b is the area of the pore bottoms; d_p is the PAA thickness, d_b is the barrier layer thickness, and ε_0 and ε are the permittivities of the vacuum and alumina [18].

Analyzing the proposed equivalent circuit helps us to define optimum parameters of cathodic and anodic pulses.

During cathodic pulse, two phenomena may be observed: (i) outer parts of pores may close due to metal deposition, and (ii) electrolyte may deplete within pores by metal cations. It is necessary to solve Faraday's equation in the integral form presented below to estimate the duration of these two processes:

$$m = \frac{MQ}{zF} = \frac{M}{zF} \int i(t) dt = \frac{MU}{zFR} \int \exp\left(-\frac{t}{RC}\right) dt \\ = \frac{M}{zF} UC \left(1 - \exp\left(-\frac{t}{RC}\right)\right), \quad (2)$$

where M is the molar mass of oxidized or reduced substance, z is the number of electrons involved in metal reduction reaction, F is the Faraday's constant, and R is the resistance of insulator. The current in (2) is determined by transients that depend on capacity of PAA/electrolyte system.

To prevent pore closing, the duration of cathodic pulse should not exceed the time of full pore closing (t_{cp}). The

closing of pores occurs when thickness of metal film h deposited at outer part of PAA becomes higher than the average radii of pores r_p . Such thickness is defined by the following equation:

$$r_p = h = \frac{m}{\rho S_{ox}} = \frac{M}{zF\rho S_{ox}} UC_p \left(1 - \exp\left(-\frac{t_{cp}}{R_p C_p}\right) \right), \quad (3)$$

where U_c is the amplitude of cathodic pulse, and R_p is the resistance of porous layer.

Thus the time of pore closing is equal to

$$t_{cp} = -R_p C_p \ln\left(1 - \frac{z\rho F n S_{ox} r_p}{M U_c C_p}\right), \quad (4)$$

where ρ is the density of metal, n is the number of pores at oxidized surface, and r_p is the pore radius.

On the other hand, it is necessary to prevent depletion of electrolyte by metal ions within pores. Otherwise, it is impossible to reach desired filling of pores by metal. Consumption of metal cations is controlled by the total capacitance of interface between inner surface of pores and electrolyte (C_Σ). Simple geometry estimations show that C_Σ is determined by the following equation:

$$C_\Sigma = C_b + \frac{4\varepsilon\varepsilon_0(d_p - d_b)\pi r_p}{d_p + d_b}. \quad (5)$$

Taking geometry of pores into account and neglecting the mass transfer it is possible to find relation between the number of ions within one pore and the duration of cathodic pulse that determines the time of pore depletion t_{dp} :

$$V = (d_p - d_b)S_b = \frac{Q}{zFC_{Me^{z+}}} = \frac{UC}{zFC_{Me^{z+}}} \left(1 - \exp\left(-\frac{t_{db}}{R_b C_\Sigma}\right) \right), \quad (6)$$

i.e.,

$$t_{db} = -R_b C_\Sigma \ln\left(1 - \frac{n z F C_{Me^{z+}} (d_p - d_b) \pi r_p^2}{U_c C_\Sigma}\right), \quad (7)$$

where $C_{Me^{z+}}$ is the density of ions of metal in electrolyte, V is the volume of single pore, and R_b is the resistance of barrier layer.

Comparing (4) and (7) shows that t_{db} is one degree more than t_{cp} for the used geometries of pores and electrolyte concentrations. Thus, the process of pore closing determines the rate of pore filling by metal.

It is obvious that consequent anodic dissolution of metal deposited at outer part of PAA is necessary for continuous pore filling. As in the case of cathodic deposition, an anodic

Table 1 Pulse electrodeposition regimes used for various metals

Metal	Cathodic impulse		Anodic impulse	
	t_{cp} (ms)	U_c (V)	t_a (ms)	U_a (V)
Cooper	4	10	36	3
Silver	3	10	37	2
Cadmium	2	10	38	4
Indium	1.5	10	38.5	4
Zinc	0.5	10	39	4
Cobalt	1	10	39	5
Nickel	1.5	10	38.5	5

dissolution of metal occurs more often at outer part of PAA. However, parameters of the anodic pulse must be chosen when taking into account incomplete dissolution of metal from bottom part of pores. Simple analysis shows that this requirement may be satisfied if the used anodic pulse amplitude is lower than the cathodic one. From this point of view, duration of anodic pulse can be estimated by the equation

$$t_a = -R_p C_p \ln\left(1 - \frac{z\rho F n S_p h}{M U_a C_p}\right), \quad (8)$$

where U_a is the amplitude of anodic pulse. To dissolve undesired metal film from outer part of PAA and to keep partially metal deposit at the bottom part of pores, the anodic pulse must be chosen from two to three times lower amplitude and from ten to forty times longer duration in comparison with cathodic pulse parameters that were presented by estimations presented in Table 1.

Table 1 summarizes the results of optimum cathodic and anodic pulse parameters estimated for various metals according to (4) and (8). In all cases, the values of $d_p = 10 \mu\text{m}$, $d_b = 8 \text{ nm}$, $S_{ox} = 5.15 \times 10^3 \text{ nm}^2$, and $S_b = 1.6 \times 10^3 \text{ nm}^2$ are used according to the results obtained from known parameters of PAA formed in 40 g/l oxalic acid aqueous solution under $j = 10 \text{ mA/cm}^2$ and $T = 25^\circ\text{C}$ during 40-min anodization [9]. The resistivity of anodic alumina oxide used is $3 \times 10^{11} \text{ Ohm cm}$ [18]. The value of $U_c = 10 \text{ V}$ has been chosen according to maximum output power of the used pulse generator.

In work [19], when using the pulsed mode of metal deposition in the pores of alumina, due to higher resistance of the electrolyte than the deposited metal, a decrease in the homogeneity of the deposited nanowires. In contrast to [19], where the authors have used the assumption that the nanowires grow up from the bottom of the pores, this paper takes into account the fact that the metal deposition occurs at both the bottom and the walls of the pores, leading to its encapsulation. During anode pulse with defined amplitude and duration, the layer of metal is completely dissolved on top of pores and partially dissolved at the bottom. By our opinion,

Fig. 3 Structures Cu/PAA formed by pulsed electrodeposition under optimum regimes, presented in Table 1 (a), using electrodeposition with longer cathodic pulse (b), and using longer anodic pulse (c)

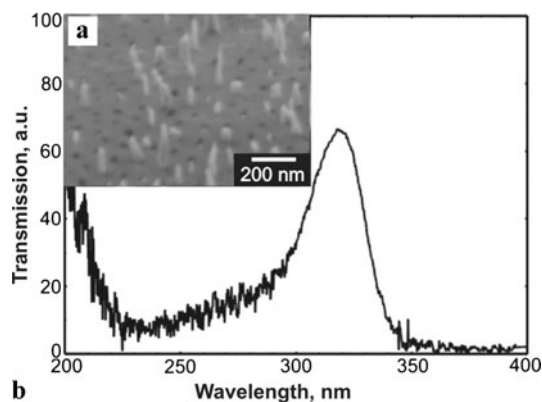
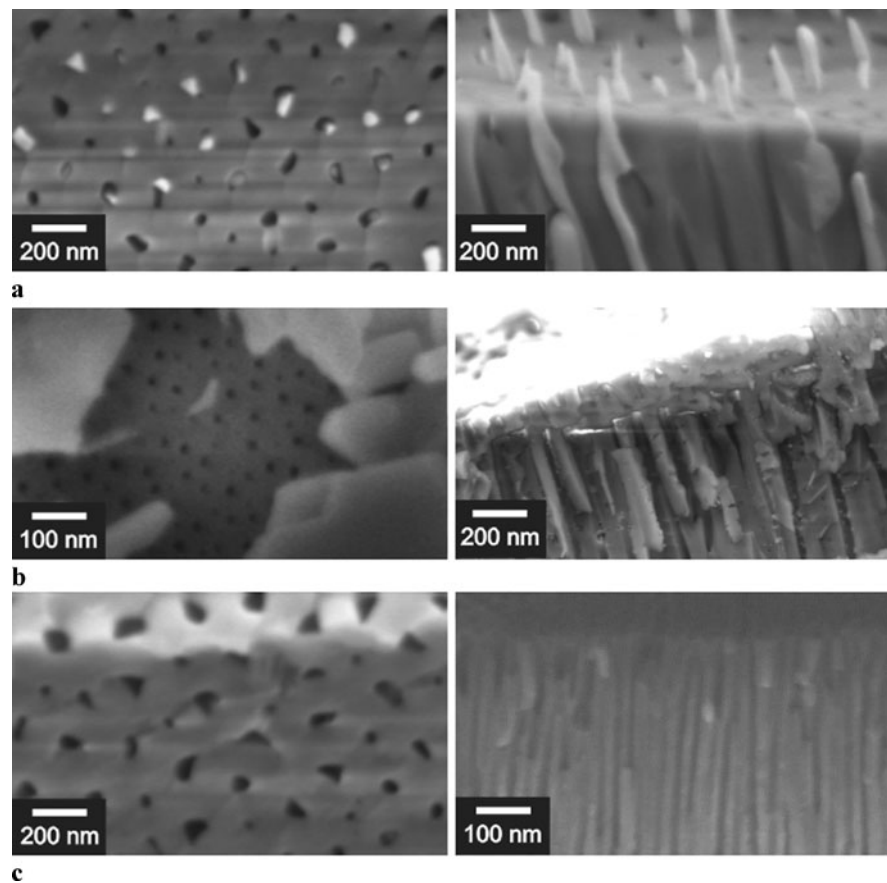


Fig. 4 Cross-section SEM-microphotography (a) and optical transmission spectrum (b) of structure Ag/PAA structure

the proposed mechanism explains increasing of deposition homogeneity.

For confirming adequacy of the developed model, various metal/PAA structures were investigated. Figure 3 shows Cu/PAA structures formed under different pulsed regimes.

When longer cathodic pulse was applied, metal deposit could not be dissolved completely under anodic pulse (Fig. 3b). Supplying longer anodic pulse results in metal dis-

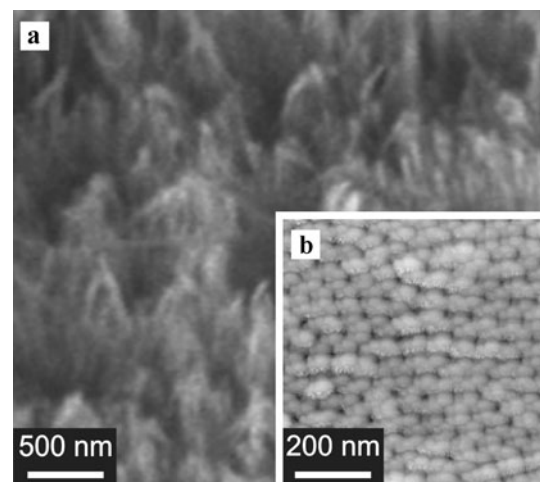


Fig. 5 SEM image of cobalt nanowires after PAA removing (a) and AFM—image of cobalt filled PAA (b)

solution within pores (Fig. 3c). Pulsed electrodeposition of other metals occurred in the same manner.

To confirm suitability of our approach to other metals, we investigated Ag/PAA and Co/PAA structures deposited under regimes presented in Table 1.

Figure 4 shows the transmission spectrum and SEM cross-section image of Ag/PAA structure. Ag fills PAA con-

formly that allows us to observe a resonant transmission peak at about 320-nm wavelength.

Successful pore filling by Co is demonstrated in Fig. 5. Image structures presented at the SEM were formed by PAA dissolution after Co-pulsed electrodeposition. Analogous results were obtained for Ni, Cd, Zn, and In nanowires and confirmed by SEM, AES, and XRD measurements not mentioned in this paper.

4 Conclusion

The attention of this work has been focused on optimizing and improving the process of pulsed electrodeposition of metal nanowires into porous anodic alumina. Utilizing the simple equivalent circuit containing parallel RC components showed that pore closing by metal deposited at outer part of porous film is always predominant. On the basis of this important finding, the optimum procedure of pulsed electrodeposition was proposed. The procedure consists of two consequential steps:

- (i) Taking the type of deposited metal and the geometry PAA film, i.e., thickness of porous and barrier parts of the PAA, and porosity and average diameter of pores into account, the time of pore closing is determined under the applied voltage pulse.
- (ii) To dissolve undesired metal film from outer part of PAA and to keep partially metal deposit at the bottom part of pores, the anodic pulse must be chosen from two to three times lower amplitude and from ten to forty times longer duration in comparison with cathodic pulse parameters.

The developed approach allowed us to perform conformal pore filling by various metals.

Acknowledgements We gratefully acknowledge Russian Basic Research Foundation for the partial financial support of this research (Grants No. 09-08-00775-a and No. 09-08-12197-ofi_m). We also thank Dr. A. Belaidi, Hahn-Meitner Institute, Berlin, for assistance in SEM imaging of investigated nanostructures.

References

1. D. Al Mawlawi, N. Coombs, M. Moskovits, *J. Appl. Phys.* **70**, 4421 (1991)
2. F. Li, R.M. Metzger, W.D. Doyle, *IEEE Trans. Magn.* **33**, 3715 (1997)
3. A.A. Tager, J.M. Xu, M. Moskovits, *Phys. Rev. B* **55**, 4530 (1997)
4. F.E. Kruijs, K. Nielsch, H. Fissan, B. Rellinghaus, E.F. Wasserman, *Appl. Phys. Lett.* **73**, 547 (1998)
5. E. Wäckelgård, *J. Phys., Condens. Matter* **8**, 5125 (1996)
6. C.N.R. Rao et al., *Prog. Solid State Chem.* **31**, 5 (2003)
7. A.P. Li, F. Muller, A. Birner, K. Nielsch, U. Gosele, *J. Appl. Phys.* **84**, 6023 (1998)
8. G. Patermarakis, K. Moussoutzakis, *Corros. Sci.* **44**, 1737 (2002)
9. H. Masuda, H. Yamada, M. Satoh, H. Asoh, M. Nakao, T. Tamamura, *Appl. Phys. Lett.* **71**, 2770 (1997)
10. A. Jagminas, S. Lichušina, M. Kurtinaitienė, A. Selskis, *Appl. Surf. Sci.* **211**, 194 (2003)
11. C.X. Gao, Q.F. Liu, D.S. Xue, *J. Mater. Sci. Lett.* **21**, 1781 (2002)
12. D. Routkevitch, T. Bigioni, M. Moskovits, J.M. Xu, *J. Phys. Chem.* **100**, 14037 (1996)
13. A. Heilmann, N. Teuscher, P. Gumbsch, Patent: DE10349471
14. S.Z. Chu, K. Wada, S. Inoue, S. Todoroki, *Electrochim. Acta* **48**, 3147 (2003)
15. K. Nielsch, F. Müller, A.-P. Li, U. Gösele, *Adv. Mater.* **12**, 582 (2000)
16. A.N. Belov, S.A. Gavrilov, V.I. Shevyakov, in *Physics, Chemistry and Application of Nanostructures: Reviews and Short Notes to Nanomeeting 2007* (2007), p. 447
17. F. Keller, M.S. Hunter, D.L. Robinson, *J. Electrochem. Soc.* **100**, 411 (1953)
18. R.K. Potucek, R.G. Rateick Jr., V.I. Birss, *J. Electrochem. Soc.* **153**, B304 (2006)
19. G. Sauer, G. Brehm, S. Schneider, K. Nielsch, R.B. Wehrspohn, J. Choi, H. Hofmeister, U. Gosele, *J. Appl. Phys.* **91**, 3243–3247 (2002)